European Journal of Mechanics B/Fluids 28 (2009) 397–404

Contents lists available at ScienceDirect

European Journal of Mechanics B/Fluids

www.elsevier.com/locate/ejmflu

Dipole-wall collision in a shallow fluid

A.R. Cieślik *, R.A.D. Akkermans, L.P.J. Kamp, H.J.H. Clercx, G.J.F. van Heijst

Fluid Dynamics Laboratory, Department of Physics, Eindhoven University of Technology, P.O. Box 513, 5600 MB Eindhoven, The Netherlands

ARTICLE INFO

Article history:
Received 28 February 2008
Received in revised form 21 October 2008
Accepted 21 October 2008
Available online 1 November 2008

Keywords:
Dipole
Vortex dynamics
Wall
Collision

ABSTRACT

Recent experiments on a freely evolving dipolar vortex in a homogeneous shallow fluid layer have clearly shown the importance of vertical secondary flows on top of the primary horizontal motion. The present contribution focuses on the interaction of such a dipolar vortex with a sidewall. Accurate measurements of the three velocity components in a single horizontal plane have been performed using the Stereoscopic Particle Image Velocimetry (SPIV) technique. The experimental results, supported by numerical simulations, indicate that the complex vertical structure of a shallow-layer dipole becomes even more complex during the collision process. The observed growth of the kinetic energy associated with enhanced vertical motion pinpoints the strong discrepancies between vortex-wall interactions in shallow fluid layers and in purely two-dimensional wall-bounded turbulence.

1. Introduction and motivation

Motivated by geophysical applications, various laboratory experiments have been performed in which fluid flow was made to behave in a quasi-two-dimensional (Q2D) manner in a number of different ways: by applying rotation, e.g. [1], density stratification, e.g. [2], and geometrical constraints, like in a soap film [3]. Experiments in shallow fluid layers also belong to this category, where the shallowness of the fluid is commonly believed to lead to Q2D flows by inhibiting vertical velocities [4,5]. In such Q2D flow systems one often encounters monopolar and dipolar vortex structures [6], and even higher-mode structures have been found. In this paper we will focus on the dynamics of a dipolar vortex in a shallow fluid layer.

A two-dimensional (2D) model for such a dipole was developed by Chaplygin and Lamb, now labeled as the Lamb–Chaplygin model, see [7]. This 2D model has been used to initialize numerical simulations of dipole-wall collisions [8] and to interpret the experimental results, obtained in both one- and two-layer systems, see [4,5] and [9]. Only recently, accurate measurements of the full three-dimensional (3D) flow field have revealed a very complex structure of an electromagnetically generated dipole in a homogeneous shallow fluid layer, with strong vertical motions, see [10,11,13]. In [10,13] the three velocity components have been measured in horizontal planes at different levels in the shallow fluid. In [11] accurate PIV measurements, with in particular the transverse vorticity in the vertical symmetry plane, have been presented. Also, less complex (but still three-dimensional) motions have been measured recently in the case of a dipolar vortex created in a linearly stratified salt solution [12].

Akkermans et al. [13], among other results, described the relaxation process, i.e. the exchange of momentum between the horizontal and vertical motions. During the forcing phase, the horizontal flow is most strongly driven close to the magnet, i.e. close to the bottom. As soon as the forcing is switched off, the horizontal flow close to the bottom is immediately reduced due to bottom friction. Because of the cyclostrophic balance between the swirling horizontal flows inside the two vortex cores, this relaxation of the horizontal flow will lead to a redistribution of the vertical pressure gradient and therefore also to a relaxation of the vertical flow that is driven by this gradient. This relaxation process was found to be of generic character, i.e. independent of the particular forcing method used here.

In the studies [10] and [12] the influence of lateral boundaries on the dynamics of the propagating dipolar vortex was ignored. The behaviour of dipoles approaching solid walls or obstacles has been studied by assuming 2D or Q2D flow behaviour, both by 2D numerical simulations [8] and by Q2D experiments in a linearly stratified salt solution [14]. Similarly, in laboratory experiments on Q2D turbulence in a confined shallow-fluid domain the influence of the lateral no-slip walls on the overall flow evolution was largely disregarded, see [15,16], under the assumption that boundary effects only play a marginal role in the overall flow evolution. Only recently the role played by lateral boundaries has gained more attention, from both an experimental and a numerical point of view, see [17,25] and references therein.

The behaviour of a purely 2D dipole colliding frontally with a no-slip wall is well-understood from numerical simulations [8,24]. When the dipolar vortex approaches a no-slip wall a thin boundary layer is formed, containing large-amplitude vorticity with signs op-

* Corresponding author.
E-mail address: A.R.Cieslik@tue.nl (A.R. Cieślik).

0997-7546/$ – see front matter
doi:10.1016/j.euromechflu.2008.10.002

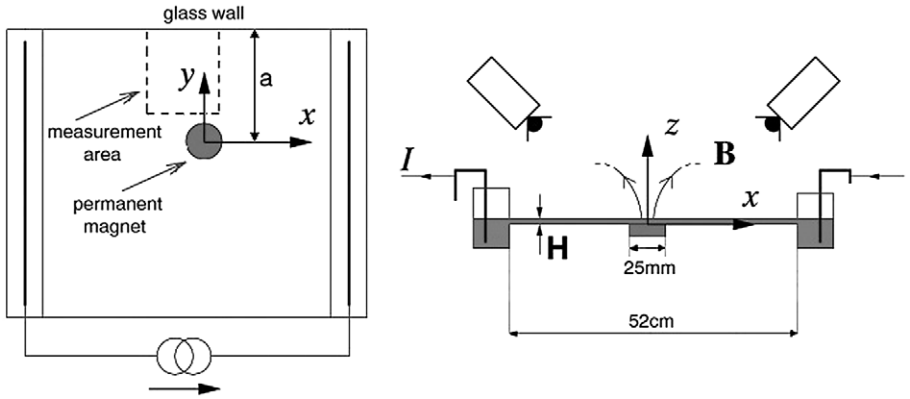

Fig. 1. A sketch of the experimental arrangement; Left: top view, Right: side view.

posite to that of the dipole halves. The wall vorticity is responsible for the subsequent separation of the dipole halves during the collision, resulting in two asymmetric dipoles, which rebound from the wall. The asymmetric secondary dipoles will propagate along curved loops towards the original symmetry axis of the dipole and they either hit the wall again or they undergo a head-on collision. In the latter case of such a collision the dipoles may show 'partner exchange', resulting in two new dipoles, where the bigger dipole moves towards the wall and the smaller one moves away in the opposite direction. This collision behaviour was also observed in laboratory experiments in a linearly stratified fluid [18]. However, numerical simulations by Orlandi [8] show that different scenarios are possible.

In the present paper we report on an experimental study of a dipolar vortex structure in a shallow fluid layer colliding with a no-slip wall. By using a Stereo PIV technique, we have been able to determine the 3D structure of the flow field. In addition, the experimental results are compared with 3D numerical simulations of the Navier–Stokes equation.

The paper is organized as follows. Section 2 gives a brief outline of the experimental setup, together with the numerical method used. Experimental results of a dipolar vortex colliding with a solid sidewall are presented in Section 3. Section 4 presents the results of numerical simulations. Finally, the main results are summarized in Section 5.

2. Experimental and numerical techniques

The experimental facility consists of a horizontal square tank 52×52 cm^2 containing a layer of a sodium chloride solution (NaCl, 24%Brix) of thickness H. Underneath the bottom plate (thickness 1 mm) of the tank a single permanent magnet is positioned. This magnet has a circular-disc shape, a diameter of 25 mm and a thickness of 5 mm, and it produces a magnetic field strength of the order of 1 tesla. The magnet is assumed to be uniformly magnetized along its axial direction. Two electrode plates are mounted on opposite sides of the container and are connected to a power supply. Application of a constant current I, in combination with the magnetic field, gives rise to a Lorentz force acting on the fluid, leading to a dipolar vortex motion in the shallow fluid layer. The fluid motion is described with respect to a Cartesian coordinate system, with the origin on the bottom of the tank and above the centre of the magnet. The z-axis coincides with the axis of the magnet, while the x-axis is parallel to the current direction, see Fig. 1. Our experimental setup is the same as in [10] and similar to the arrangement used by some other investigators, e.g. Dolzhanskii et al. [19], Paret et al. [16] and Boffetta et al. [20].

In order to measure all three velocity components of the velocity field, the fluid was seeded with passive particles with diameters between 250–300 microns. During the experiment these particles are illuminated by a horizontal laser light sheet with a thickness of 1 mm, entering the measurement area through the glass side wall of the tank (see Fig. 1). Positions of the illuminated particles were recorded by two cameras viewing from two different angles. The Stereoscopic Particle Image Velocimetry (SPIV) method was used to obtain the three velocity components in a single horizontal plane, see [10] for details. The measurement area was 75×100 mm^2, as indicated by the dashed rectangle in Fig. 1. The spatial resolution for flow measurements in this area is slightly below 2 mm.

Table 1
Parameter values of the performed experiments: H is the total fluid depth, a is the distance between the centre of the magnet and the wall, I is the electrical current, and h_{LS} denotes the measurement level.

H [mm]	a [mm]	I [A]	h_{LS} [mm]
11.4	85	8	5.0
11.4	60	8	5.0
11.4	35	8	5.0
11.4	–	8	5.0
6.2	85	5.6	3.5
6.2	60	5.6	3.5
6.2	35	5.6	3.5
6.2	–	5.6	3.5

Eight experiments were performed with different fluid depths H, different distances a of the centre of the magnet to the wall, and various current strengths I. In each experiment we measured all three components of the velocity vector at one horizontal level (h_{LS}) above the bottom: $h_{LS} = 5$ mm for $H = 11.4$ mm experiments and $h_{LS} = 3.5$ mm for $H = 6.2$ mm experiments. For a summary of all parameter values of all conducted experiments we refer to Table 1. This paper reports in detail on only one experiment done in a fluid layer with depth $H = 11.4$ mm, with the magnet-wall distance $a = 60$ mm. However, similarities and differences between this experiment and the other experiments will be discussed briefly at the end of this paper.

Complementary to these experiments we have performed numerical simulations solving the full 3D Navier–Stokes equation for an incompressible fluid subjected to an electromagnetic forcing $\vec{f}_L$:

$$\vec{f}_L = \vec{j} \times \vec{B}, \tag{1}$$

where $\vec{j}$ represents the current density and $\vec{B}$ the magnetic field of the permanent magnet. A uniformly distributed current density $\vec{j} = j_0 \vec{e}_x$ is assumed. The permanent magnet is modeled by a stack of circular current loops that generate the azimuthally uniform magnetic field induced by the magnet. The magnetic field of a single current loop is known in terms of elliptic integrals [21] and the magnetic field of a stack of current loops is then easily obtained by superposing a number of such particular magnetic field contributions.

The magnitude of the uniform magnetization current is not exactly known and therefore the strength of the electromagnetic forcing is known in analytical form up to a multiplicative constant. In the simulations presented in this paper this constant was obtained through the matching of the maximum vertical vorticity at the end of the forcing stage with that observed experimentally.

The numerical simulation of a forced dipolar vortex colliding with the wall was performed with a finite-element code [22]. The boundary conditions were taken as in the experiments: a no-slip condition at the bottom and the lateral wall and a stress-free condition at the upper boundary. The upper boundary is taken to be rigid, which implies that surface deformations are not taken into account. This approach was validated for the freely evolving dipole [10]. Under the assumption of symmetry with respect to the vertical plane $x = 0$, the computations were carried out for only one dipole half, while applying a symmetry condition at the symmetry plane of the dipole. The additional simulation, carried out in a full domain and without imposing the symmetry condition, showed minor differences with respect to the half-domain simulation.

For a typical run the computational domain is divided into approximately 50,000 mesh elements with a very fine mesh near the wall and near the no-slip bottom, especially close to the magnet, where the dipole is created and where the gradients in the flow are expected to be largest. Additionally, the resolution in the vertical direction was twice the resolution in the horizontal direction. Convergence of the solution was checked in a simulation with a refined mesh.

3. Dipole evolution during collision

In order to clearly identify the effect of a solid wall on the approaching dipole, two experiments were performed: one with and the other without any lateral wall, while all other parameters were kept fixed.

3.1. Dipole-wall collision

The evolution of the dipolar vortex during its collision with the lateral no-slip wall is shown by displaying the vertical velocity in Fig. 2 (left column) and the vertical vorticity in Fig. 3 (left column). As the dipole reaches the wall (Fig. 2a) we observe a characteristic strong vertical motion in front of it. This vertical motion is organized in a roll of positive (upwelling) and negative (downwelling) velocities, and was reported before, e.g. [4] and [23]. This roll, essentially a vortex tube containing vorticity (ω_x) in the x-direction, will be referred to as the frontal recirculation (FR).

As the collision continues (Fig. 2b, c), the FR disappears and a rapid narrowing of the downward motion area in the direction perpendicular to the wall sets in. This narrowing implies stretching of the vortex tube in the direction parallel to the wall, resulting in the enhancement of the x-component of the vorticity (ω_x) and hence of the vertical velocities. At $t = 2$ s (Fig. 2c) the FR has disappeared and now the area of the downward motion between the wall and the dipole cores is narrowed too, again resulting in enhanced vertical velocities. At the late stage of the collision ($t = 4$ s, Fig. 2d), when the rebound of the dipole is in progress, the vertical motion inside the dipole is still clearly visible. By comparing Fig. 2b, c and d it is seen that the downward motion inside the core of this dipole half (marked by black circles in Fig. 2) gradually moves towards the wall and from the symmetry axis.

At the beginning of the dipole collision process (at $t = 1$ s, Fig. 3a) one observes the production of oppositely signed vertical vorticity (ω_z) at the wall. Also a band of oppositely signed vertical vorticity develops in the frontal part of the dipole (marked by an ellipse in Fig. 3a) and at the back of the dipole (marked by kidney-shaped contours in Fig. 3b, c).

3.2. Experiments without the wall

Fig. 2 (right column; vertical velocity) and Fig. 3 (right column; vertical vorticity) show the results of the experiment without the wall. The observations from this experiment at two crucial instants of time ($t = 1.6$ s and $t = 2$ s) will be compared with those of the wall experiment at the same instants of time.

Fig. 2e shows the velocity field at $t = 1.6$ s for the freely propagating dipole. Comparing this plot with Fig. 2b one observes that during the dipole-wall collision the cross-sectional area of the FR is narrowed while the dipole approaches the wall. In the freely evolving dipole the FR decays slightly until $t = 2$ s (Fig. 2f). Additionally, the area of strong downward and upward motion inside the dipole is rather unaffected by the interaction with the wall. However, the upward and downward motion concentrated in the two elongated bands on the side and the back of the vortex core (marked by kidney-shaped regions in Fig. 2) is observed to be enhanced by the collision, especially at later times.

Fig. 3e shows the vertical vorticity field at $t = 1.6$ s for the freely propagating dipole. Comparing the strength of the vertical component of the vorticity ω_z inside the kidney-shaped contours in Fig. 3b, c (with wall) with that in Figs. 3e, f (no wall) reveals that the collision leads to an intensification of ω_z in these regions. In contrast, in the no-wall experiment we observe fragmentation and subsequent decay of ω_z at the rear of the dipole.

In order to quantify the degree to which the wall collision leads to enhanced three-dimensionality we computed the time evolution of the size of the cross-sectional area of downward motion in the FR for the two experiments (Fig. 4a). Moreover, the evolution of the mean vertical velocity inside this area, $\langle w_{FR} \rangle$ (Fig. 4b) has been determined. In the two plots in Fig. 4 we can identify three regimes: (I) after the forcing is switched off (at time $t = 0$ s) the FR cell is being built up progressively, resulting in a monotonically increasing area and vertical velocity; (II) around $t = 0.7$ s this growth of area and magnitude of downward motion comes to a hold and subsequently vertical motion starts to decay; (III) around $t = 0.9$ s the collision sets in and we observe a discrepancy between the evolution of the FR in the two experiments. Obviously, the area of downward motion is being narrowed between the wall and the approaching dipole and vertical velocities are amplified there, as can be observed in Fig. 4b. In the case of the freely evolving dipole no enhancement of vertical motions is observed and the decay of the downward motion in the FR continues.

4. Results of 3D numerical simulations

Fig. 5 shows the results of 3D numerical simulations of the dipolar structure colliding with the wall. The evolution of the x-component of the vorticity (left column of Fig. 5) in the vertical symmetry plane $x = 0$ clearly shows the roll structure in front of the dipole. The vertical cross-sectional plots clearly reveal the downward motion near the wall at $t = 1$ s and 1.6 s. As the collision proceeds, this cell is narrowed in the direction perpendicular to the wall, as is clearly visible in Fig. 5c for $t = 2$ s. The associated vortex tube stretching in the direction parallel to the wall (i.e. in x-direction) then leads to enhanced downward motion close to the wall, as was also observed in the experiment. In the very late stage of the collision process (Fig. 5d) this FR cell has been pushed away completely, and the internal band of positive ω_x has arrived at the wall, implying locally upward motion. This scenario corresponds with experimentally observed vertical velocities near the wall, see Fig. 2 (left column).

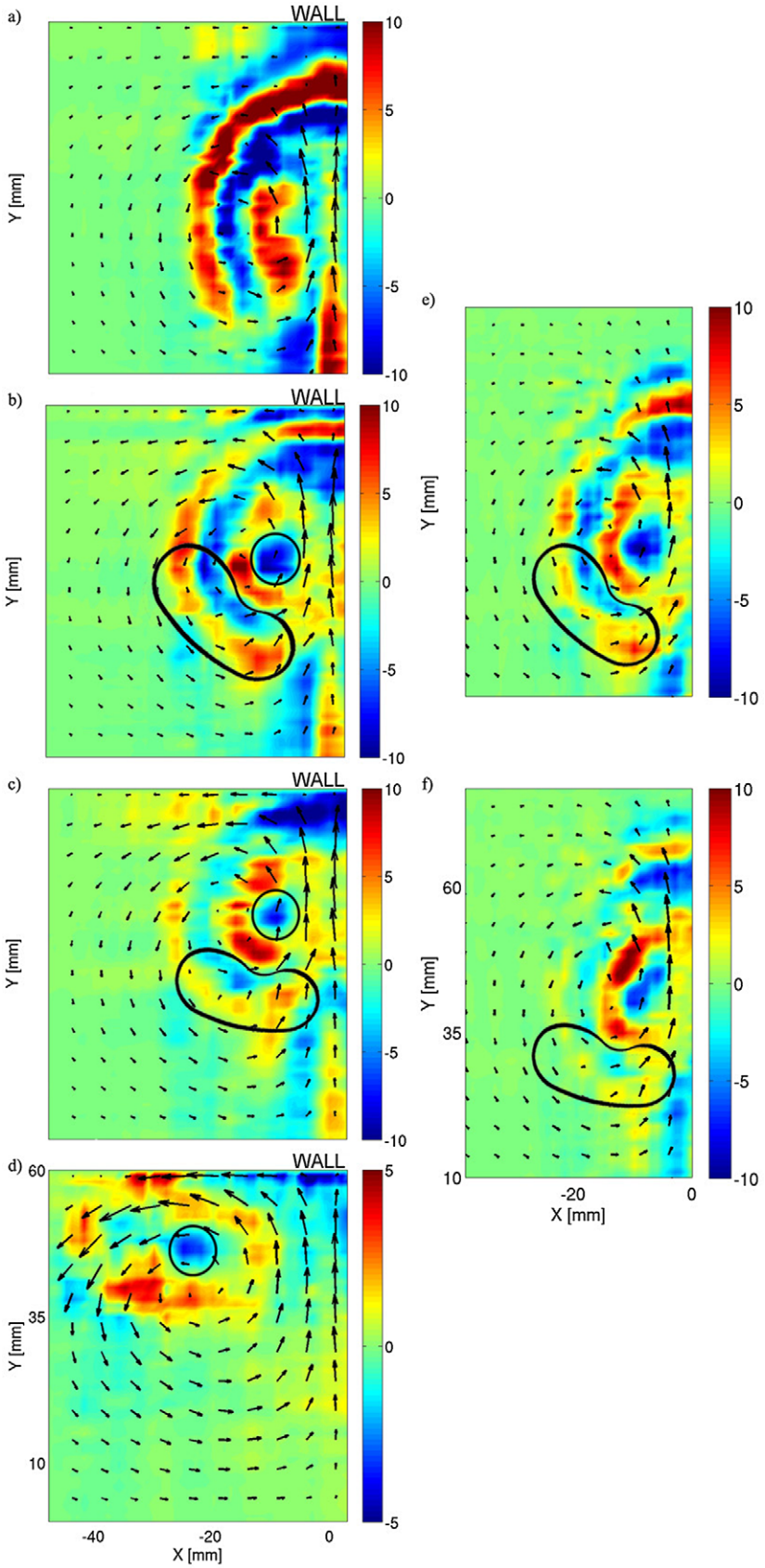

Fig. 2. (Color online) Snapshots of vertical velocity w (in mm/s) obtained from experiments of the dipole-wall collision (left column) and from experiments with a freely evolving dipole (right column) at $t = 1$ s (a), $t = 1.6$ s (b, e), $t = 2$ s (c, f) and $t = 4$ s (d). Arrows denote the horizontal velocities in the plane $z = 5$ mm. The same scaling of x and y coordinates was used. The downward motion inside the core of the dipole half is indicated by the black circles. The vertical motion in the rear of the dipole is marked by the kidney-shaped contours.

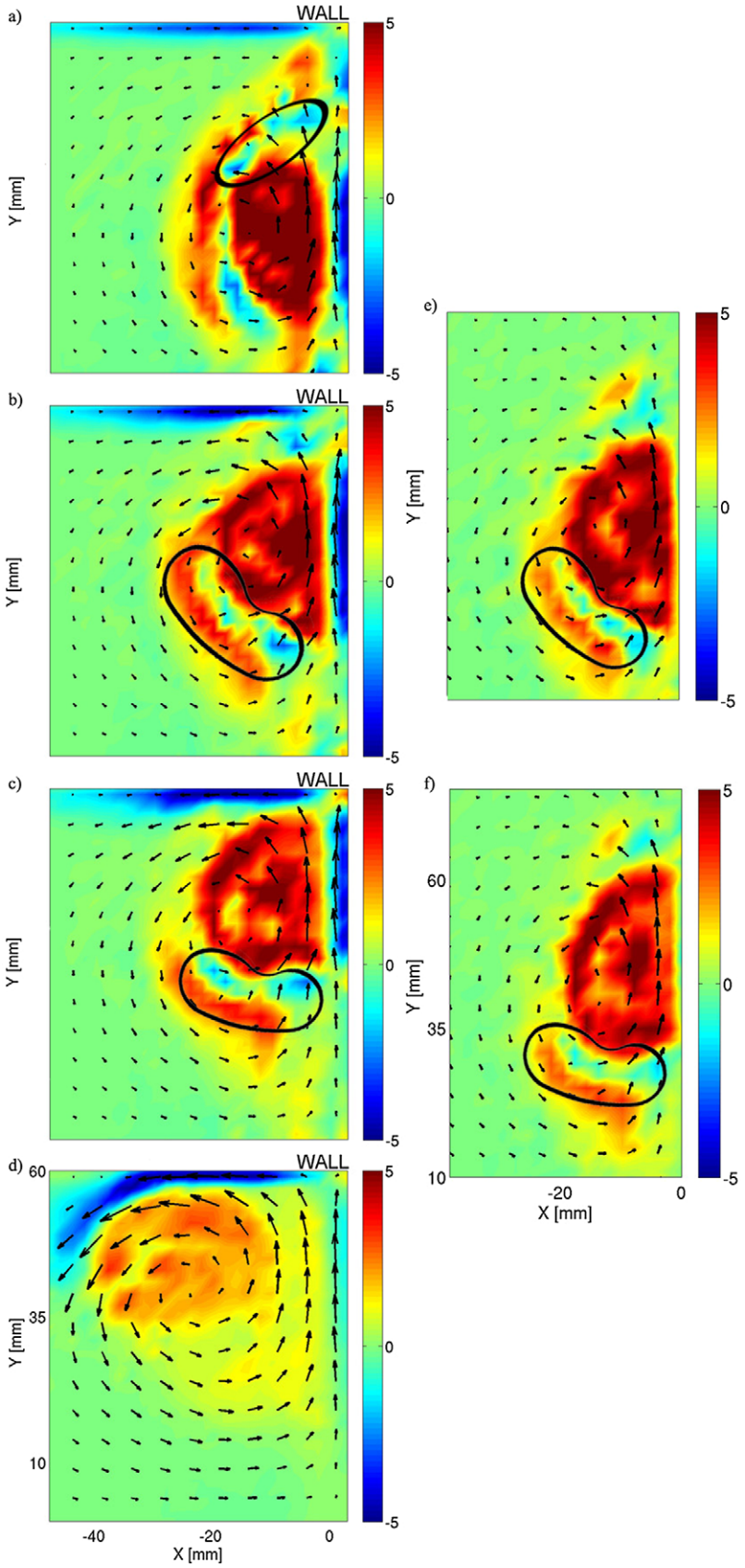

Fig. 3. (Color online) Snapshots of vertical vorticity ω_z (in s^{-1}) obtained from experiments of the dipole-wall collision (left column) and from experiments with a freely evolving dipole (right column) at $t = 1$ s (a), $t = 1.6$ s (b, e), $t = 2$ s (c, f) and $t = 4$ s (d). Arrows denote the horizontal velocities in the plane $z = 5$ mm. The same scaling of x and y coordinates was used. The presence of bands with positive and negative vertical vorticity in the rear of the dipole is indicated by the kidney-shaped contours. The elliptical contour in (a) marks negative vertical vorticity in front of the dipole.

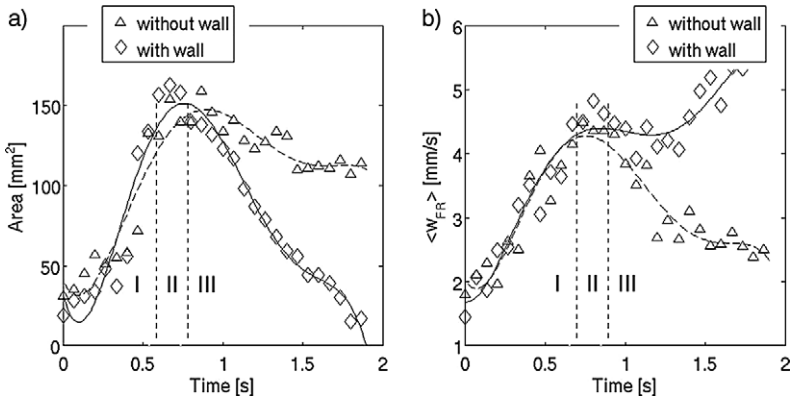

Fig. 4. Evolution of the downward motion in the FR in the experiment with and without the wall. The area of downwelling (a) and mean vertical velocity in this area (b). Curves represent 5th order polynomial fit to the experimental data. Dashed vertical lines indicate the three different stages of the dipole evolution.

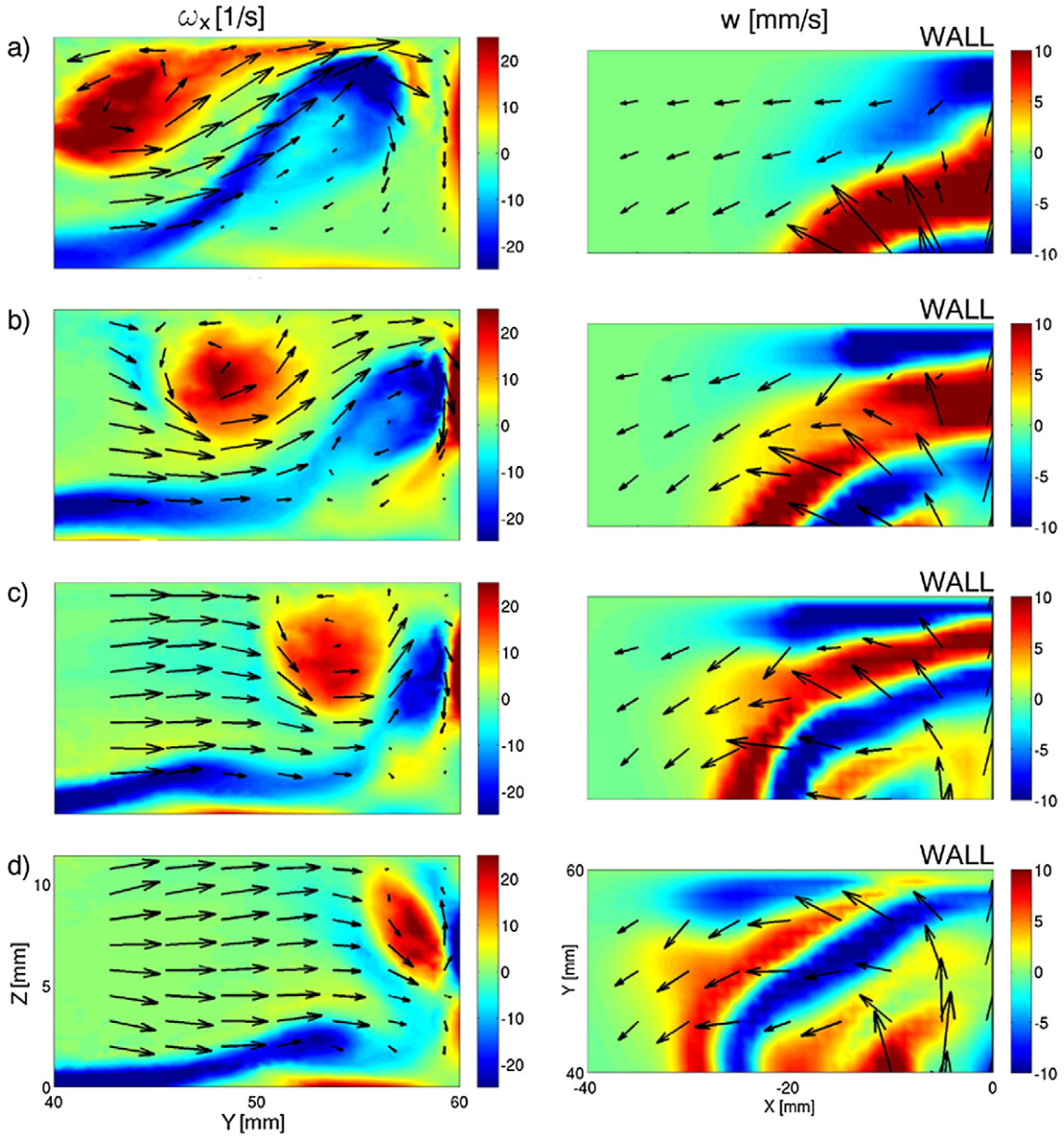

Fig. 5. (Color online) Snapshots of the x-component of the vorticity ω_x (left column) in the vertical symmetry plane $x = 0$ and vertical velocity w (right column) in the horizontal plane $z = 5$ mm obtained from simulations of the dipole-wall collision at time $t = 1$ s (a), $t = 1.6$ s (b), $t = 2$ s (c) and $t = 2.5$ s (d). Colors represent the magnitude of the plotted quantities (see color bars for numerical values), while the arrows represent the velocity field in the cross-sectional plane. The solid wall lies at $y = 60$ mm.

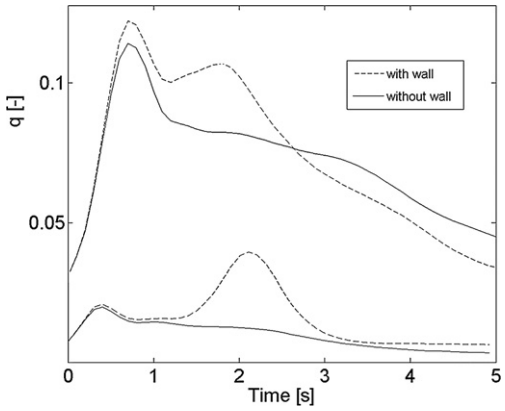

Fig. 6. Ratio of vertical to horizontal kinetic energy q. Comparison between simulation with (Fig. 5) and without the wall for $H = 11.4$ mm (upper plots) and $H = 6.2$ mm (lower plots).

However, especially at later stages of the flow evolution, the differences between experimental and numerical results are becoming more apparent. Here we conjecture that these discrepancies are due to surface deformations, which are not allowed for in the simulations. This conjecture is based on the fact that the 3D numerical simulations do reproduce quite well the experimental results as far as the free evolution of the dipole is concerned (see also [13]), thus excluding any type of free surface deformation as a source of vertical motions.

In order to quantify the increase of three-dimensionality during the collision of the dipolar structure with the wall, we performed a second set of numerical simulations without any wall, with the other parameter settings unchanged. Three-dimensionality of the flow field is quantified here in terms of the ratio q of the instantaneous kinetic energies associated with the vertical flow and those associated with the horizontal flow,

$$q = \frac{\iiint w^2\,dx\,dy\,dz}{\iiint (u^2+v^2)\,dx\,dy\,dz} \tag{2}$$

where u, v and w denote the x, y, z-components of the velocity, respectively. Fig. 6 shows the evolution of the kinetic energy ratio q as computed from the numerical results of the two simulations. The first maximum in these curves is to be associated with the relaxation of the horizontal to vertical energy ratio as described in the Introduction. The second maximum is related to the collision of the dipole with the wall and can be attributed to the enhanced downward motion close to the wall.

In contrast to what could be expected, the collision in the shallower layer ($H = 6.2$ mm) leads to a much larger relative increase of the vertical velocities (Fig. 6, lower plots): the ratio q has doubled. This remarkably different behaviour can be explained as follows. Fig. 7 shows the vertical velocities in the horizontal planes $z = 5$ mm for $H = 11.4$ mm and $z = 3$ mm for $H = 6.2$ mm. Fig. 7 (left column) indicates a very complex vertical flow inside the dipole with strong upwelling and downwelling in the whole velocity field of the dipole. This implies that only a small portion of the vertical kinetic energy is associated with the FR. In contrast, in the shallower layer ($H = 6.2$ mm, Fig. 7, right column) vertical motion is present only in the spanwise roll in front of the dipole. This implies that a large portion of the vertical kinetic energy is strongly influenced during the dipole-wall collision.

5. Conclusions

In this paper we have investigated experimentally and numerically the interaction of a shallow-layer dipole with a lateral wall. Three-dimensional numerical simulations show good agreement

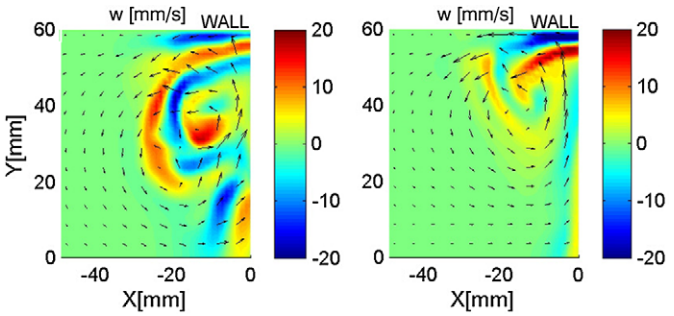

Fig. 7. (Color online) Snapshots of the numerically computed vertical velocity w in the horizontal planes $z = 5$ mm for $H = 11.4$ mm (left column) and $z = 3$ mm for $H = 6.2$ mm (right column) at time $t = 2$ s.

with the experimental results during the first stage of the collision process when the influence of the wall is still negligible. Once the dipolar structure hits the wall we observe a significant increase of three-dimensionality, in the form of enhanced downward motion close to the wall. The discrepancies between the experimental results and the numerical simulations are attributed to free surface deformations, which are not accounted for in the simulations. These deformations may have a pronounced influence on the generation of additional three-dimensionality near lateral walls.

The increasing three-dimensionality in the dipole colliding with the wall has been observed in all the experiments performed (see Table 1). When the distance between the magnet and the wall becomes quite small (e.g. $a = 35$ mm), the structure of the colliding dipole is very different from the one shown in Fig. 2 (left column). Specifically we then observe an upwelling rather than a downwelling area in front of the dipole when it collides with the wall.

Remarkably, the influence of the wall on the vertical motion inside the dipolar vortex is much more significant in the shallower experiment. This is because at the time of the collision the vertical velocities are confined only to the frontal circulation roll.

Acknowledgements

Two of the authors (A.R.C. and R.A.D.A.) gratefully acknowledge the financial support from the Dutch Foundation for Fundamental Research on Matter (FOM). L.J.A. van Bokhoven is gratefully acknowledged for providing the SPIV code.

References

[1] G.J.F. van Heijst, R.C. Kloosterziel, Tripolar vortices in a rotating fluid, Nature 338 (1989) 569–571.
[2] J.B. Flór, G.J.F. van Heijst, An experimental study of dipolar vortex structures in a stratified fluid, J. Fluid Mech. 279 (1994) 101–133.
[3] Y. Couder, C. Basdevant, Experimental and numerical study of vortex couples in two-dimensional flows, J. Fluid Mech. 173 (1986) 225–251.
[4] D. Sous, N. Bonneton, J. Sommeria, Turbulent vortex dipoles in a shallow water layer, Phys. Fluids 16 (2004) 2886–2898.
[5] D. Sous, N. Bonneton, J. Sommeria, Transition from deep to shallow water layer: formation of vortex dipoles, Eur. J. Mech. B/Fluids 24 (2005) 19–32.
[6] G.J.F. van Heijst, J.B. Flór, Dipole formation and collisions in a stratified fluid, Nature 340 (1989) 212–215.
[7] V.V. Meleshko, G.J.F. van Heijst, On Chaplygin's investigation of two-dimensional vortex structures in an inviscid fluid, J. Fluid Mech. 272 (1994) 157–182.
[8] P. Orlandi, Vortex dipole rebound from a wall, Phys. Fluids A 2 (1990) 1429–1436.
[9] Y.D. Afanasyev, V.N. Korabel, Starting vortex dipoles in a viscous fluid: Asymptotic theory, numerical simulations and laboratory experiments, Phys. Fluids 16 (2004) 3850–3858.
[10] R.A.D. Akkermans, L.P.J. Kamp, H.J.H. Clercx, G.J.F. van Heijst, Intrinsic three-dimensionality in electromagnetically driven shallow flows, Europhys. Lett. 83 (2008) 24001.

[11] J. Albagnac, P. Brancher, O. Eiff, L. Lacaze, F. Moulin, Vortex dipole evolution in shallow water, in: Mixing of Coastal, Estuarine and Riverine Shallow Flows, Euromech Colloquium 501, 8–11 June 2008, Ancona, Italy.
[12] O. Praud, A.M. Fincham, The structure and dynamics of dipolar vortices in a stratified fluid, J. Fluid Mech. 544 (2005) 1–22.
[13] R.A.D. Akkermans, A.R. Cieslik, L.P.J. Kamp, R.R. Trieling, H.J.H. Clercx, G.J.F. van Heijst, The three-dimensional structure of an electromagnetically generated dipolar vortex in a shallow fluid layer, Phys. Fluids 20 (2008), in press.
[14] R. Verzicco, J.B. Flór, G.J.F. van Heijst, P. Orlandi, Numerical and experimental study of the interaction between a vortex and a circular cylinder, Exp. Fluids 18 (1995) 153–163.
[15] M.K. Rivera, W.B. Daniel, S.Y. Chen, R.E. Ecke, Energy and enstrophy transfer in decaying two-dimensional turbulence, Phys. Rev. Lett. 90 (2003) 104502.
[16] J. Paret, M.C. Jullien, P. Tabeling, Vorticity statistics in the two-dimensional enstrophy cascade, Phys. Rev. Lett. 83 (1999) 3418–3421.
[17] G.J.F. van Heijst, H.J.H. Clercx, D. Molenaar, The effects of solid boundaries on confined two-dimensional turbulence, J. Fluid Mech. 554 (2006) 411–431.
[18] G.J.F. van Heijst, J.B. Flór, Laboratory experiments on dipole structures in a stratified fluid, in: J.C.J. Nihoul, B.M. Jamart (Eds.), Mesoscale/Synoptic Coherent Structures in Geophysical Turbulence: Proceedings of the 20th International Liège Colloquium on Ocean Hydrodynamics, Elsevier Science Publishing, Amsterdam, The Netherlands, 1989, pp. 591–608.
[19] F.V. Dolzhanskii, V.A. Krymov, D.Yu. Manin, An advanced experimental investigation of quasi-two-dimensional shear flows, J. Fluid Mech. 241 (1992) 705–722.
[20] G. Boffetta, A. Cenedese, S. Espa, S. Musacchio, Effects of friction on 2d turbulence: An experimental study of the direct cascade, Europhys. Lett. 71 (2005) 590–596.
[21] J. Schwinger, Classical Electrodynamics, Perseus Books, Cambridge, 1998.
[22] http://www.comsol.com/.
[23] J.-C. Lin, M. Ozgoren, D. Rockwell, Space–time development of the onset of a shallow-water vortex, J. Fluid Mech. 485 (2003) 33–66.
[24] H.J.H. Clercx, C.H. Bruneau, The normal and oblique collision of a dipole with a no-slip boundary, Computers and Fluids 35 (2006) 245–279.
[25] H.J.H. Clercx, G.J.F. van Heijst, Two-dimensional Navier–Stokes turbulence in bounded domains, Appl. Mech. Rev. (2009), in press.